Nuclear Responses for Double Beta Decay and Muon Capture

Lotta Jokiniemi

Department of Physics, University of Jyväskylä
MEDEX'19, Prague 27-31 May, 2019

May 29, 2019

JYVÄSKYLÄN YLIOPISTO
UNIVERSITY OF JYVÄSKYLÄ

Outline

Motivation

- $\beta\beta$-decays challenging to study both experimentally and theoretically
  $\rightarrow$ Both charge-exchange reactions and muon capture offer a detour to study them.

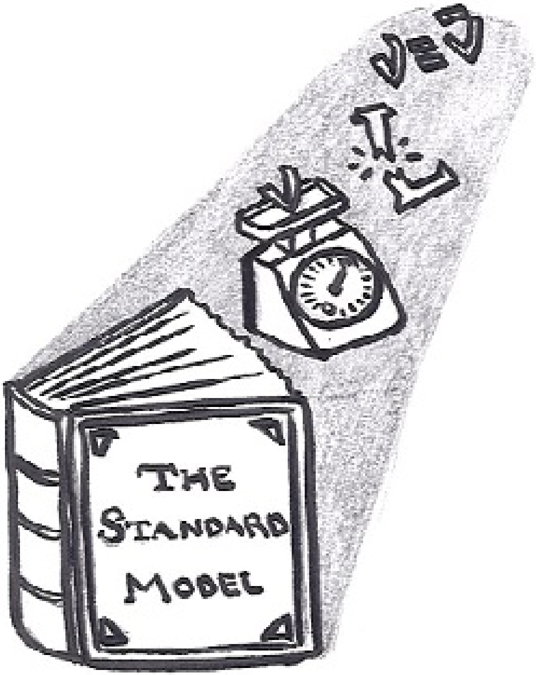

Motivation

- $\beta\beta$-decays challenging to study both experimentally and theoretically
  $\rightarrow$ Both charge-exchange reactions and muon capture offer a detour to study them.
- Reliable description of the intermediate states essential for probing the half-lives of $0\nu\beta\beta$-decay.

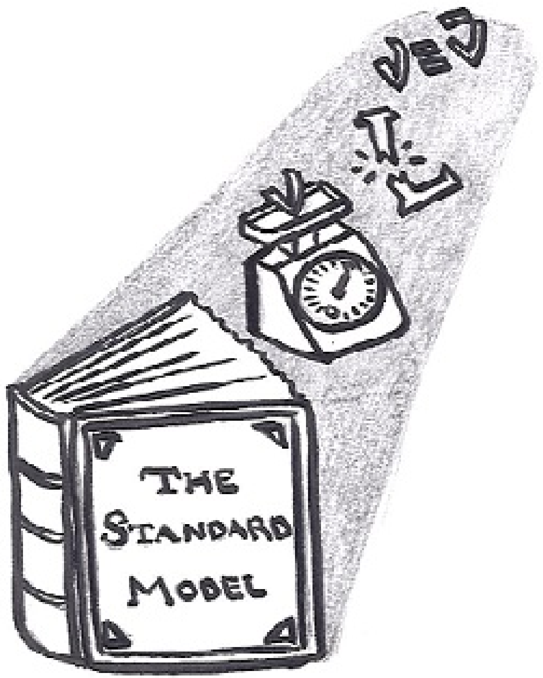

Motivation

- $\beta\beta$-decays challenging to study both experimentally and theoretically
  $\rightarrow$ Both charge-exchange reactions and muon capture offer a detour to study them.
- Reliable description of the intermediate states essential for probing the half-lives of $0\nu\beta\beta$-decay.
- Physics beyond the Standard Model!

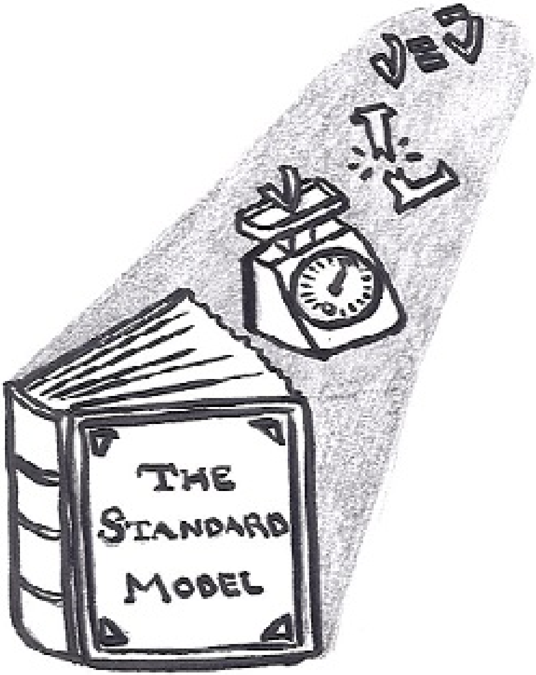

Charge-Exchange Reactions as a Probe

- $\beta\beta$ decays take place between two even-even nuclei of the isobaric chain trough the virtual states of the intermediate odd-odd nucleus.

Charge-Exchange Reactions as a Probe

- $\beta\beta$ decays take place between two even-even nuclei of the isobaric chain trough the virtual states of the intermediate odd-odd nucleus.
- $0\nu\beta\beta$-decay runs trough all possible multipolarities J^π of the intermediate nucleus (whereas $2\nu\beta\beta$ runs only trough 1^+ states).

Charge-Exchange Reactions as a Probe

- $\beta\beta$ decays take place between two even-even nuclei of the isobaric chain trough the virtual states of the intermediate odd-odd nucleus.
- $0\nu\beta\beta$-decay runs trough all possible multipolarities J^π of the intermediate nucleus (whereas $2\nu\beta\beta$ runs only trough 1^+ states).
- Intermediate J^π states of $0\nu\beta\beta$ decay can be studied by utilising the corresponding $\beta^-(\beta^+)$ transitions of the mother(daughter) nucleus.

Charge-Exchange Reactions as a Probe

- $\beta\beta$ decays take place between two even-even nuclei of the isobaric chain trough the virtual states of the intermediate odd-odd nucleus.
- $0\nu\beta\beta$-decay runs trough all possible multipolarities J^π of the intermediate nucleus (whereas $2\nu\beta\beta$ runs only trough 1^+ states).
- Intermediate J^π states of $0\nu\beta\beta$ decay can be studied by utilising the corresponding $\beta^-(\beta^+)$ transitions of the mother(daughter) nucleus.
- The energetics and strength distributions of these reactions were studied using pnQRPA theory with large no-core single-particle bases.

Charge-Exchange Reactions as a Probe

- $\beta\beta$ decays take place between two even-even nuclei of the isobaric chain trough the virtual states of the intermediate odd-odd nucleus.
- $0\nu\beta\beta$-decay runs trough all possible multipolarities J^π of the intermediate nucleus (whereas $2\nu\beta\beta$ runs only trough 1^+ states).
- Intermediate J^π states of $0\nu\beta\beta$ decay can be studied by utilising the corresponding $\beta^-(\beta^+)$ transitions of the mother(daughter) nucleus.
- The energetics and strength distributions of these reactions were studied using pnQRPA theory with large no-core single-particle bases.
- The aim is to probe the particle-hole parameter g_{ph} by fitting it to experimental data.

$0\nu\beta\beta$ Decay and CEX Reactions in the $A = 76$ Triplet

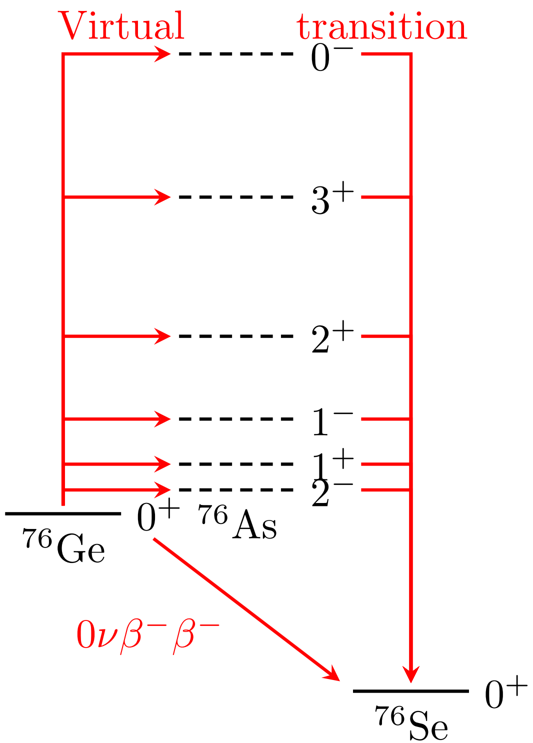

Figure 1: $0\nu\beta\beta$ transition.

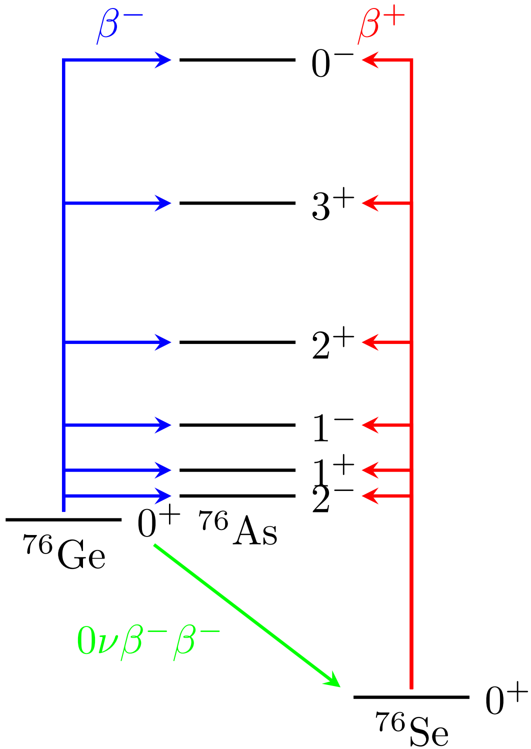

Figure 2: Charge-exchange reactions.

Results: Fitting the Particle-Hole Parameter to Experiments

- Measurements on isovector spin-dipole $J^{\pi} = 2^{-}$ transitions led by Prof. Hiro Ejiri at RCNP, University of Osaka and by Prof. Dieter Frekers at University of Muenster.

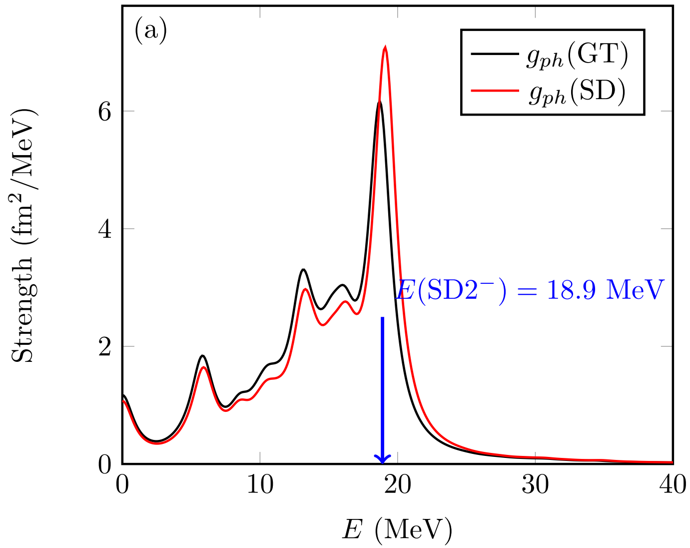

Figure 3: Isovector spin-dipole $J^{\pi} = 2^{-}$ spectra for $A = 76$ [1].

[1] L. Jokiniemi *et al.*, *Phys. Rev. C*, **98**, 024608 (2018).

Results: Fitting the Particle-Hole Parameter to Experiments

- Measurements on isovector spin-dipole $J^\pi = 2^-$ transitions led by Prof. Hiro Ejiri at RCNP, University of Osaka and by Prof. Dieter Frekers at University of Muenster.
- The particle-hole parameter g_{ph} traditionally fitted to Gamow-Teller giant resonances $\rightarrow$ How about fitting g_{ph} to spin-dipole giant resonances, instead?

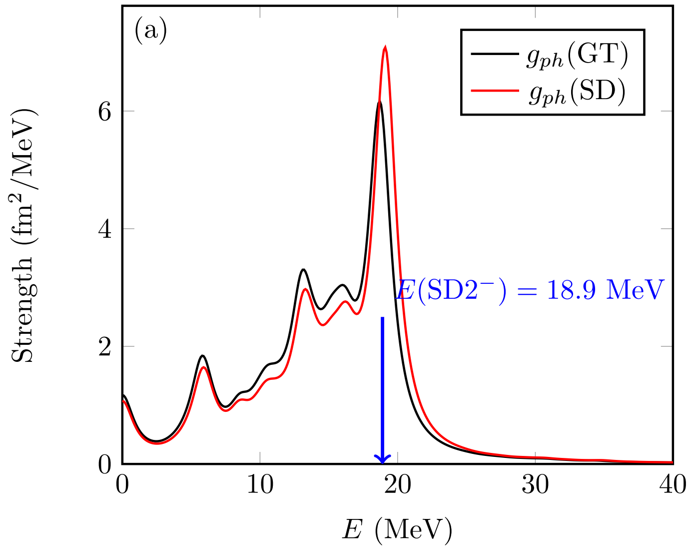

Figure 3: Isovector spin-dipole $J^\pi = 2^-$ spectra for $A = 76$ [1].

[1] L. Jokiniemi *et al.*, *Phys. Rev. C*, **98**, 024608 (2018).

Results: The Values of g_{ph}

Table 1: Parameters of the pnQRPA calculations for various $0\nu\beta\beta$ decaying nuclei.

Nucleus	$E(\mathrm{SD}2^-)$ (MeV)	$E(\mathrm{GT})$ (MeV)	$g_{\mathrm{ph}}(2^-)$	$g_{\mathrm{ph}}(\mathrm{GT})$
^{76}Ge	18.9 ± 1.0	11.4 ± 0.5	1.2 ± 0.3	1.03 ± 0.13
^{96}Zr	22 ± 1.0	12.7 ± 0.5	0.8 ± 0.2	0.84 ± 0.09
^{100}Mo	19.7 ± 1.0	12.2 ± 0.5	1.0 ± 0.2	1.19 ± 0.08
^{116}Cd	20.5 ± 1.0	13.0 ± 0.5	1.07 ± 0.09	0.85 ± 0.13
^{128}Te	21.3 ± 1.0	13.8 ± 0.5	1.9 ± 0.2	1.40 ± 0.09
^{130}Te	21.7 ± 1.0	14.2 ± 0.5	1.9 ± 0.2	1.36 ± 0.09
^{136}Xe	22.1 ± 1.0	14.6 ± 0.5	0.9 ± 0.2	1.18 ± 0.08

Results: $0\nu\beta\beta$ Matrix Elements Using Spin-Dipole Data

Different models

1. $g_{\rm ph} = g_{\rm ph}(\rm GT)$ for all J^π.[2]
2. $g_{\rm ph} = g_{\rm ph}(\rm SD2^-)$ for $J^\pi = 2^-$, for the rest $g_{\rm ph} = g_{\rm ph}(\rm GT)$.
3. $g_{\rm ph} = g_{\rm ph}(\rm GT)$ for $J^\pi = 1^+$, for the rest $g_{\rm ph} = g_{\rm ph}(\rm SD2^-)$.

Nuclear transition	Model	$M^{(0\nu)}$
$^{76}\rm Ge \longrightarrow {}^{76}Se$	1	6.9 ± 0.3
	2	6.8 ± 0.3
	3	6.6 ± 0.4
	1,small[2]	6.54
$^{96}\rm Zr \longrightarrow {}^{96}Mo$	1	5.3 ± 0.2
	2	5.3 ± 0.2
	3	5.5 ± 0.4
	1,small[2]	4.47
$^{100}\rm Mo \longrightarrow {}^{100}Ru$	1	5.54 ± 0.10
	2	5.55 ± 0.11
	3	5.9 ± 0.4
	1,small[2]	4.98
$^{116}\rm Cd \longrightarrow {}^{116}Sn$	1	5.7 ± 0.2
	2	5.7 ± 0.2
	3	5.39 ± 0.13
	1,small[2]	4.93
$^{128}\rm Te \longrightarrow {}^{128}Xe$	1	5.52 ± 0.15
	2	5.47 ± 0.15
	3	4.9 ± 0.3
	1,small[2]	5.74
$^{130}\rm Te \longrightarrow {}^{130}Xe$	1	4.77 ± 0.12
	2	4.72 ± 0.12
	3	4.1 ± 0.2
	1,small[2]	5.27
$^{136}\rm Xe \longrightarrow {}^{136}Ba$	1	3.72 ± 0.09
	2	3.76 ± 0.10
	3	4.1 ± 0.3
	1,small[2]	3.50

[2] J. Hyvärinen and J. Suhonen, *Phys. Rev. C*, **91**, 024613 (2015).

Muon Capture as a Probe

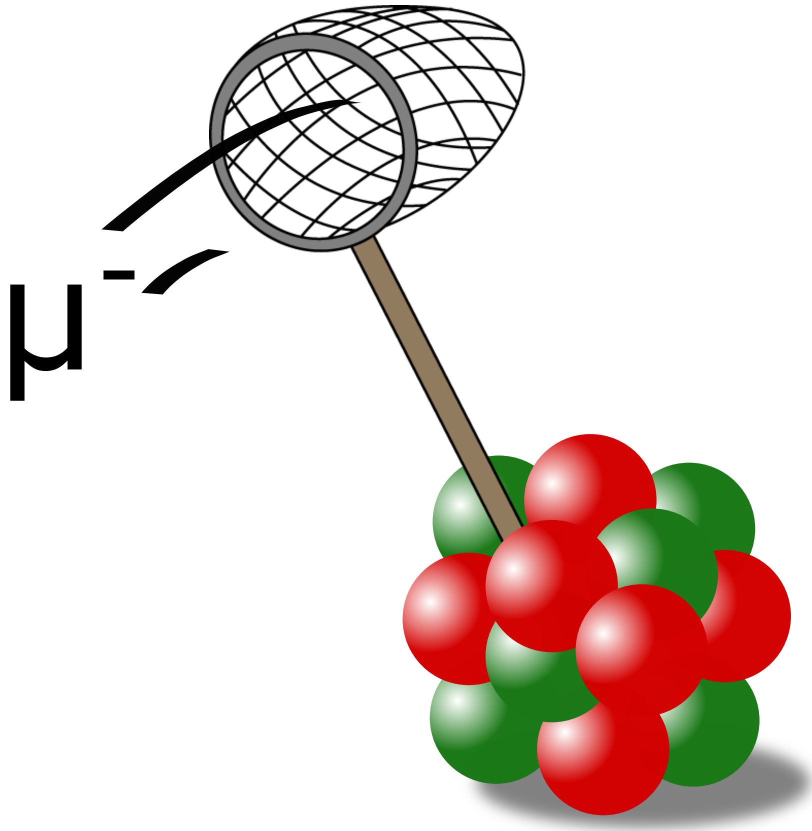

Figure 4: Very schematic figure of a muon capture.

Ordinary Muon Capture (OMC)

OMC

$$\mu^- + (A, Z) \rightarrow \nu_\mu + (A, Z-1)$$

- Weak interaction process with high energy release and large momentum transfer.

Ordinary Muon Capture (OMC)

OMC

$\mu^- + (A, Z) \rightarrow \nu_\mu + (A, Z-1)$

- Weak interaction process with high energy release and large momentum transfer.
- Energy release is about 100 MeV, of which the largest fraction is donated to the neutrino.

Ordinary Muon Capture (OMC)

OMC

$$\mu^- + (A, Z) \rightarrow \nu_\mu + (A, Z - 1)$$

- Weak interaction process with high energy release and large momentum transfer.
- Energy release is about 100 MeV, of which the largest fraction is donated to the neutrino.
- Large mass of the captured muon allows forbidden transitions and high excitation energies of the final state.

Muon Capture Formalism

- OMC rates based on Morita-Fujii formalism [3].

[3] M. Morita, and A. Fujii, Phys. Rev. **118**, 606 (1960).
[4] H. Primakoff, Rev. Mod. Phys. **31**, 802 (1959).

Muon Capture Formalism

- OMC rates based on Morita-Fujii formalism [3].
- Muonic screening is taken into account by the Primakoff method [4].

[3] M. Morita, and A. Fujii, Phys. Rev. **118**, 606 (1960).
[4] H. Primakoff, Rev. Mod. Phys. **31**, 802 (1959).

Muon Capture Formalism

- OMC rates based on Morita-Fujii formalism [3].
- Muonic screening is taken into account by the Primakoff method [4].
- Capture rate to a J^{π} final state can be written as

$$W = 8\left(\frac{Z_{\text{eff}}}{Z}\right)^4 P(\alpha Z m'_{\mu})^3 \frac{2J_f+1}{2J_i+1}\left(1-\frac{q}{m_{\mu}+AM}\right)q^2\,, \qquad (1)$$

where

- A is the mass number of the nuclei,
- $Z(Z_{\text{eff}})$ the (effective) atomic number of the initial nucleus,
- $J_i(J_f)$ the angular momentum of the initial (final) nucleus,
- M the average nucleon mass,
- m_{μ} the bound muon mass,
- α the fine-structure constant, and
- q the Q value of the OMC.

---

[3] M. Morita, and A. Fujii, Phys. Rev. **118**, 606 (1960).

[4] H. Primakoff, Rev. Mod. Phys. **31**, 802 (1959).

- The Q value of the OMC can be written as

$$q = (m_\mu - W_0)\left(1 - \frac{m_\mu - W_0}{2(M_f + m_\mu)}\right) , \tag{2}$$

where $W_0 = M_f - M_i + m_e + E_X$, and

  - $M_f(M_i)$ is the mass of the final(initial) nucleus,
  - m_e the electron mass, and
  - E_X the excitation energy of the final state.

OMC Formalism: P Term

- The term P in Eq. (1) can be written as

$$
\begin{aligned}
P =& \frac{1}{2}\sum_{\kappa u}\Big| g_{\rm V}[0\,l\,u]S_{0u}(\kappa)\delta_{lu} + g_{\rm A}[1\,l\,u]S_{1u}(\kappa) - \frac{g_{\rm V}}{M}[1\,\bar{l}\,u\,p]S'_{1u}(-\kappa) \\
&+ \sqrt{3}\frac{g_{\rm V}q}{2M}\left(\sqrt{\frac{\bar{l}+1}{2\bar{l}+3}}[0\,\bar{l}{+}1\,u\,{+}]\delta_{\bar{l}+1,u} + \sqrt{\frac{\bar{l}}{2\bar{l}-1}}[0\,\bar{l}{-}1\,u\,{-}]\delta_{\bar{l}-1,u}\right)S'_{1u}(-\kappa) \\
&+ \sqrt{\frac{3}{2}}\left(\frac{g_{\rm V}q}{M}\right)(1+\mu_p-\mu_n)\Big(\sqrt{\bar{l}+1}W(1\,1\,u\,\bar{l}\,;1\,\bar{l}+1)[1\,\bar{l}{+}1\,u\,{+}] \\
&+ \sqrt{\bar{l}}W(1\,1\,u\,\bar{l}\,;1\,\bar{l}-1)[1\,\bar{l}{-}1\,u\,{-}]\Big)S'_{1u}(-\kappa) \\
&- \left(\frac{g_{\rm A}}{M}\right)[0\,\bar{l}\,u\,p]S'_{0u}(-\kappa)\delta_{\bar{l}u} + \sqrt{\frac{1}{3}}(g_{\rm P}-g_{\rm A})\left(\frac{q}{2M}\right) \\
&\times \left(\sqrt{\frac{\bar{l}+1}{2\bar{l}+1}}[1\,\bar{l}{+}1\,u\,{+}] + \sqrt{\frac{\bar{l}}{2\bar{l}+1}}[1\,\bar{l}{-}1\,u\,{-}]\right) \\
&\times S'_{0u}(-\kappa)\delta_{\bar{l}u}\Big|^2 ,
\end{aligned}
\tag{3}
$$

where we abbreviate $[k\,w\,u\,(^{\pm}_{p})] := \mathcal{M}[k\,w\,u\,(^{\pm}_{p})]$.

OMC Formalism: P Term

- The term P can be expanded in terms of a small quantity $1/M^2$ as $P = P_0 + P_1$, where

OMC Formalism: P Term

- The term P can be expanded in terms of a small quantity $1/M^2$ as $P = P_0 + P_1$, where
  - P_0 is obtained by neglecting terms containing $1/M^2$, and

OMC Formalism: P Term

- The term P can be expanded in terms of a small quantity $1/M^2$ as $P = P_0 + P_1$, where
  - P_0 is obtained by neglecting terms containing $1/M^2$, and
  - P_1 includes all terms of the order $1/M^2$.

OMC Formalism: P Term

- The term P can be expanded in terms of a small quantity $1/M^2$ as $P = P_0 + P_1$, where
  - P_0 is obtained by neglecting terms containing $1/M^2$, and
  - P_1 includes all terms of the order $1/M^2$.
- Original Morita-Fujii formalism included only the leading-order P_0 term

OMC Formalism: P Term

- The term P can be expanded in terms of a small quantity $1/M^2$ as $P = P_0 + P_1$, where
  - P_0 is obtained by neglecting terms containing $1/M^2$, and
  - P_1 includes all terms of the order $1/M^2$.
- Original Morita-Fujii formalism included only the leading-order P_0 term
  - This can lead to unphysical results for some weak transitions to high-lying states

OMC Formalism: P Term

- The term P can be expanded in terms of a small quantity $1/M^2$ as $P = P_0 + P_1$, where
  - P_0 is obtained by neglecting terms containing $1/M^2$, and
  - P_1 includes all terms of the order $1/M^2$.
- Original Morita-Fujii formalism included only the leading-order P_0 term
  - This can lead to unphysical results for some weak transitions to high-lying states
- We extended the formalism by adding the P_1 term in the calculations.

OMC Formalism: P_0 Term for nth Forbidden Transition:

$$
\begin{aligned}
P_0 =& g_{\rm V}^2[0\,n\,n]^2 + \frac{1}{3}g_{\rm A}^2\Big([1\,n\,n]^2 + [1\,n\,n{+}1]^2 + [1\,n{+}2\,n{+}1]^2\Big) + \frac{1}{2n+1}g_{\rm V}^2\frac{q}{M}[0\,n\,n]\Big(n[0\,n\,n\,+]\\
&+ (n+1)[0\,n\,n\,-]\Big) + \sqrt{\frac{n(n+1)}{3}}\frac{1}{2n+1}g_{\rm V}^2\frac{q}{M}(1+\mu_p-\mu_n)[0\,n\,n]\Big(-[1\,n\,n\,-]+[1\,n\,n\,+]\Big)\\
&- \sqrt{\frac{n(n+1)}{3}}\frac{1}{2n+1}g_{\rm A}g_{\rm V}\frac{q}{M}[1\,n\,n]\Big([0\,n\,n\,-]-[0\,n\,n\,+]\Big)\\
&+ \frac{1}{3}g_{\rm A}g_{\rm V}\frac{q}{M}(1+\mu_p-\mu_n)\Big\{\frac{1}{2n+1}[1\,n\,n]\Big(n[1\,n\,n\,-]+(n+1)[1\,n\,n\,+]\Big)\\
&+ \frac{1}{2n+3}\Big(\sqrt{n+2}[1\,n\,n{+}1]-\sqrt{n+1}[1\,n{+}2\,n{+}1]\Big)\Big(\sqrt{n+2}[1\,n\,n{+}1\,-]-\sqrt{n+1}[1\,n{+}2\,n{+}1\,+]\Big)\Big\}\\
&+ \frac{1}{3(2n+3)}g_{\rm A}(g_{\rm A}-g_{\rm P})\frac{q}{M}\Big(\sqrt{n+1}[1\,n\,n{+}1]+\sqrt{n+2}[1\,n{+}2\,n{+}1]\Big)\Big(\sqrt{n+1}[1\,n\,n{+}1\,-]\\
&+ \sqrt{n+2}[1\,n{+}2\,n{+}1\,+]\Big) - \frac{2}{\sqrt{3(2n+1)}}g_{\rm V}^2\frac{1}{M}[0\,n\,n]\Big(\sqrt{n}[1\,n{-}1\,n\,p]+\sqrt{n+1}[1\,n{+}1\,n\,p]\Big)\\
&- \frac{2}{3}g_{\rm A}g_{\rm V}\frac{1}{M}\Big\{\frac{1}{\sqrt{2n+3}}\Big(-\sqrt{n+2}[1\,n\,n{+}1]+\sqrt{n+1}[1\,n{+}2\,n{+}1]\Big)[1\,n{+}1\,n{+}1\,p]\\
&+ \frac{1}{\sqrt{2n+1}}[1\,n\,n]\Big(\sqrt{n+1}[1\,n{-}1\,n\,p]-\sqrt{n}[1\,n{+}1\,n\,p]\Big)\Big\}\\
&+ \frac{2}{\sqrt{3(2n+3)}}g_{\rm A}^2\frac{1}{M}\Big(\sqrt{n+1}[1\,n\,n{+}1]+\sqrt{n+2}[1\,n{+}2\,n{+}1]\Big)[0\,n{+}1\,n{+}1\,p]\\
&+ \frac{1}{12(2n+3)}\Big(\frac{g_{\rm P}q}{M}\Big)^2\Big(\sqrt{n+1}[1\,n\,n{+}1\,-]+\sqrt{n+2}[1\,n{+}2\,n{+}1\,+]\Big)^2
\end{aligned}
\tag{4}
$$

OMC Formalism: Added P_1 Term:

$$
\begin{aligned}
P_1 = & \left(\frac{g_\mathrm{A}}{M}\right)^2 [0\,n{+}1\,n{+}1]^2 + g_\mathrm{V}^2 \left(\frac{q}{2M}\right)^2 \frac{1}{2n+1}\Big(n[0\,n\,n\,+]^2 + (n+1)[0\,n\,n\,-]^2\Big) \\
& + \frac{1}{3}\left(\frac{g_\mathrm{V}}{M}\right)^2 \Big([1\,n{-}1\,n\,p]^2 + [1\,n{+}1\,n\,p]^2 + [1\,n{+}1\,n{+}1\,p]^2\Big) \\
& + \frac{1}{12}(g_\mathrm{A}^2 - 2g_\mathrm{A}g_\mathrm{P})\left(\frac{q}{M}\right)^2 \frac{1}{2n+3}\Big(\sqrt{n+2}[1\,n{+}2\,n{+}1\,+] + \sqrt{n+1}[1\,n\,n{+}1\,-]\Big)^2 \\
& + \frac{1}{12}\left(\frac{g_\mathrm{V}q}{2M}\right)^2 (1+\mu_p-\mu_n)\Big\{\frac{1}{2n+1}\Big((n+1)[1\,n\,n\,+]^2 + n[1\,n\,n\,-]^2\Big) \\
& + \frac{1}{2n+3}\Big(\sqrt{n+1}[1\,n{+}2\,n{+}1\,+] - \sqrt{n+2}[1\,n\,n{+}1\,-]\Big)^2\Big\} \\
& - \frac{1}{\sqrt{3(2n+1)}}\left(\frac{g_\mathrm{V}}{M}\right)^2 q\Big(\sqrt{n}[1\,n{-}1\,n\,p][0\,n\,n\,+] + \sqrt{n+1}[1\,n{+}1\,n\,p][0\,n\,n\,-]\Big) \\
& + \frac{1}{3}\left(\frac{g_\mathrm{V}}{M}\right)^2 q(1+\mu_p-\mu_n)\Big\{\frac{1}{\sqrt{2n+1}}\Big(\sqrt{n}[1\,n{+}1\,n\,p][1\,n\,n\,-] - \sqrt{n+1}[1\,n{-}1\,n\,p][1\,n\,n\,+]\Big) \\
& + \frac{1}{\sqrt{2n+3}}\Big(\sqrt{n+2}[1\,n{+}1\,n{+}1\,p][1\,n\,n{+}1\,-] - \sqrt{n+1}[1\,n{+}1\,n{+}1\,p][1\,n{+}2\,n{+}1\,+]\Big)\Big\} \\
& + \frac{1}{2\sqrt{3}}\left(\frac{g_\mathrm{V}q}{M}\right)^2 (1+\mu_p-\mu_n)\frac{\sqrt{n(n+1)}}{2n+1}\Big([0\,n\,n\,+][1\,n\,n\,+] - [0\,n\,n\,-][1\,n\,n\,-]\Big) \\
& + \frac{1}{\sqrt{3}}g_\mathrm{A}(g_\mathrm{A}-g_\mathrm{P})\frac{q}{M^2}\frac{1}{\sqrt{2n+3}}[0\,n{+}1\,n{+}1\,p]\Big(\sqrt{n+2}[1\,n{+}2\,n{+}1\,+] + \sqrt{n+1}[1\,n\,n{+}1\,-]\Big)
\end{aligned}
\tag{5}
$$

Muon Capture Calculations in This Study

1. Muon capture rate distribution on ^{100}Mo computed with pnQRPA, and compared with experimental data.

Muon Capture Calculations in This Study

1. Muon capture rate distribution on ^{100}Mo computed with pnQRPA, and compared with experimental data.
2. Muon capture rate distributions on the daughter nuclei of key $\beta\beta$-decay triplets, ^{76}Se, ^{82}Kr, ^{96}Mo, ^{100}Ru, ^{116}Sn, ^{128}Xe, ^{130}Xe, and ^{136}Ba, computed with pnQRPA.

Muon Capture Calculations in This Study

1. Muon capture rate distribution on ^{100}Mo computed with pnQRPA, and compared with experimental data.
2. Muon capture rate distributions on the daughter nuclei of key $\beta\beta$-decay triplets, ^{76}Se, ^{82}Kr, ^{96}Mo, ^{100}Ru, ^{116}Sn, ^{128}Xe, ^{130}Xe, and ^{136}Ba, computed with pnQRPA.
3. OMC rates compared with $0\nu\beta\beta$ matrix elements.

Results 1/3: Theoretical vs. Experimental Muon Capture Spectra in ^{100}Nb

- For the first time, OMC giant resonance was observed in ^{100}Nb [5].

[5] I. H. Hashim *et al.*, *Phys. Rev. C*, **97**, 014617 (2018).

Results 1/3: Theoretical vs. Experimental Muon Capture Spectra in ^{100}Nb

- For the first time, OMC giant resonance was observed in ^{100}Nb [5].
- OMC rate distribution to the excited states of ^{100}Nb computed and compared with the experimental strength distribution.

[5] I. H. Hashim *et al.*, *Phys. Rev. C*, **97**, 014617 (2018).

Results 1/3: Theoretical vs. Experimental Muon Capture Spectra in ^{100}Nb

- For the first time, OMC giant resonance was observed in ^{100}Nb [5].
- OMC rate distribution to the excited states of ^{100}Nb computed and compared with the experimental strength distribution.
- Involved nuclear wave functions computed with pnQRPA with large no-core single-particle bases.

[5] I. H. Hashim *et al.*, *Phys. Rev. C*, **97**, 014617 (2018).

Results 1/3: Theoretical vs. Experimental Muon Capture Spectra in ^{100}Nb

- For the first time, OMC giant resonance was observed in ^{100}Nb [5].
- OMC rate distribution to the excited states of ^{100}Nb computed and compared with the experimental strength distribution.
- Involved nuclear wave functions computed with pnQRPA with large no-core single-particle bases.
- Obtained giant resonance compared with the experimental one $\rightarrow$ Both distributions show giant resonance at around 12 MeV!

[5] I. H. Hashim *et al.*, *Phys. Rev. C*, **97**, 014617 (2018).

Results 1/3: Theoretical vs. Experimental Muon Capture Spectra in ^{100}Nb

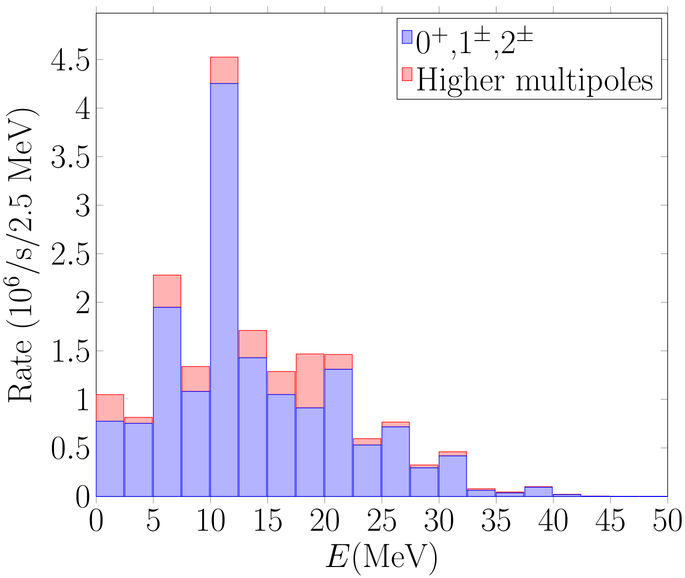

Figure 5: Theoretical muon capture rate distribution to ^{100}Nb.

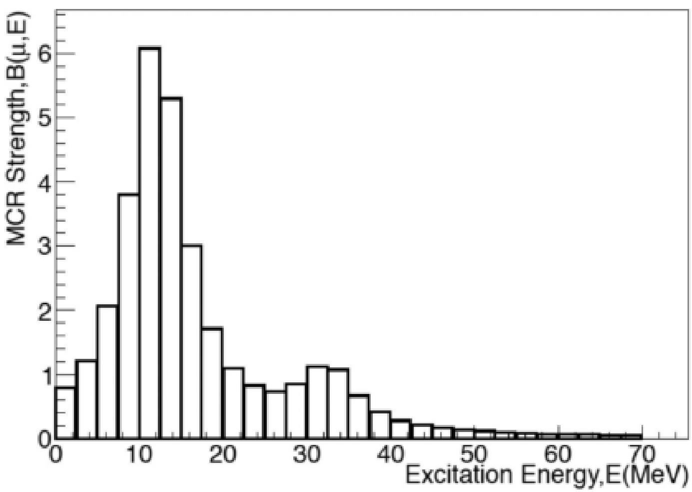

Figure 6: Experimental muon capture strength distribution to ^{100}Nb.[6]

[6] I. H. Hashim *et al.*, *Phys. Rev. C*, **97**, 014617 (2018).

Results 1/3: Theoretical vs. Experimental Muon Capture Spectra in ^{100}Nb

- Primakoff estimate for the total muon capture rate

$$W_{\mathrm{Pr.}}(A,Z) = Z_{\mathrm{eff}}^{4} X_1 \left[1 - X_2 \left(\frac{A-Z}{2A} \right) \right] , \tag{6}$$

where $X_1 = 170$ 1/s and $X_2 = 3.125$, gives $W_{\mathrm{Pr.}}(^{100}\mathrm{Mo}) = 7.7 \times 10^{6}$ 1/s.

Results 1/3: Theoretical vs. Experimental Muon Capture Spectra in ^{100}Nb

- Primakoff estimate for the total muon capture rate

$$W_{\mathrm{Pr.}}(A,Z) = Z_{\mathrm{eff}}^4 X_1 \left[1 - X_2 \left(\frac{A-Z}{2A}\right)\right] , \tag{6}$$

  where $X_1 = 170$ 1/s and $X_2 = 3.125$, gives $W_{\mathrm{Pr.}}(^{100}\mathrm{Mo}) = 7.7 \times 10^6$ 1/s.

- Total OMC rate value obtained from pnQRPA calculations (with $g_\mathrm{A} = 0.8$ and $g_\mathrm{P} = 10$) was $W_{\mathrm{tot}} = 17.7 \times 10^6$ 1/s
  $\rightarrow$ This suggests for quenched $g_\mathrm{A} \approx 0.5$!

Results 2/3: OMC Strength Functions in Intermediate Nuclei of $0\nu\beta\beta$ Decays

- OMC rates to the intermediate nuclei of neutrinoless double beta ($0\nu\beta\beta$) decays of current experimental interest are computed in the pnQRPA framework.

[7] D. Zinatulina *et al.*, Phys. Rev. C **99**, 024327 (2019).

Results 2/3: OMC Strength Functions in Intermediate Nuclei of $0\nu\beta\beta$ Decays

- OMC rates to the intermediate nuclei of neutrinoless double beta ($0\nu\beta\beta$) decays of current experimental interest are computed in the pnQRPA framework.
- The corresponding OMC (capture-rate) strength functions have been analyzed in terms of multipole decompositions.

[7] D. Zinatulina *et al.*, Phys. Rev. C **99**, 024327 (2019).

Results 2/3: OMC Strength Functions in Intermediate Nuclei of $0\nu\beta\beta$ Decays

- OMC rates to the intermediate nuclei of neutrinoless double beta ($0\nu\beta\beta$) decays of current experimental interest are computed in the pnQRPA framework.
- The corresponding OMC (capture-rate) strength functions have been analyzed in terms of multipole decompositions.
- The computed low-energy OMC-rate distribution to ^{76}As is compared with the available data of Zinatulina *et al.*[7]

[7] D. Zinatulina *et al.*, Phys. Rev. C **99**, 024327 (2019).

Results 2/3: OMC Strength Functions in Intermediate Nuclei of $0\nu\beta\beta$ Decays

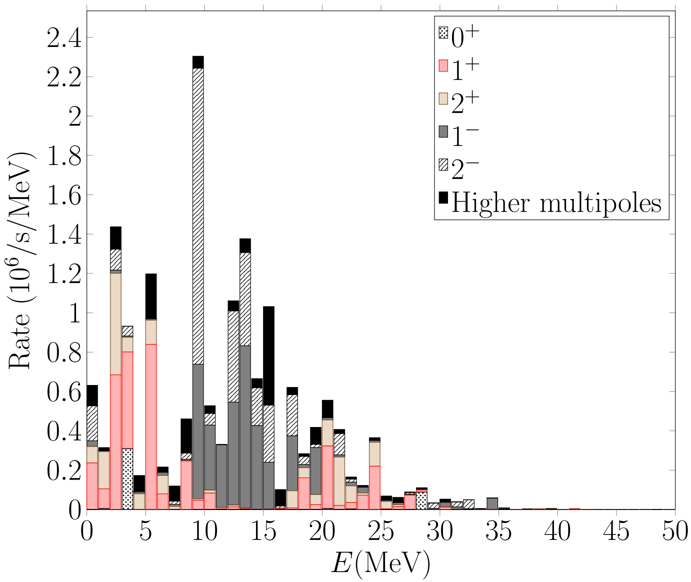

Figure 7: OMC rate distribution for $^{76}\mathrm{Se}(0^+_{\mathrm{g.s.}}) + \mu^- \rightarrow {}^{76}\mathrm{As}(J^\pi) + \nu_\mu$.

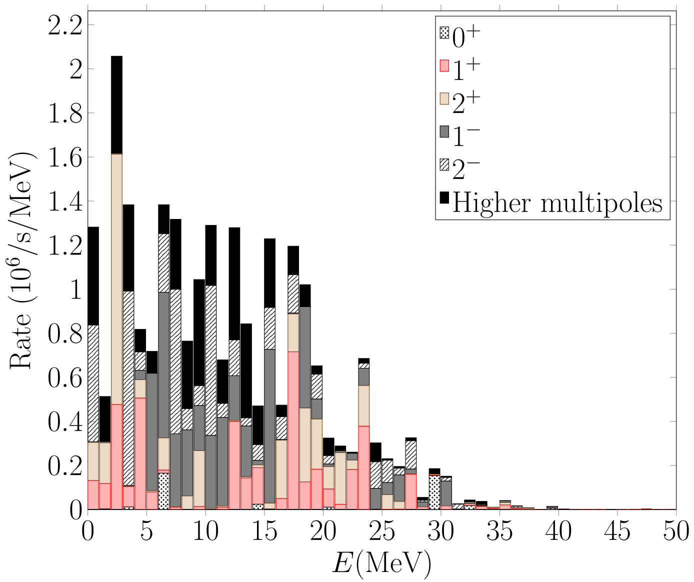

Figure 8: OMC rate distribution for $^{130}\mathrm{Xe}(0^+_{\mathrm{g.s.}}) + \mu^- \rightarrow {}^{130}\mathrm{I}(J^\pi) + \nu_\mu$.

Results 2/3: OMC Strength Functions in Intermediate Nuclei of $0\nu\beta\beta$ Decays

Table 2: The "most probable" experimental OMC strength distribution below 1.1 MeV in ^{76}As[8] compared with the corresponding pnQRPA-computed distribution. 'g.s.' means transitions to the ground state that could not be measured.

	OMC rate (1/s)	
J^π	Exp.	pnQRPA
0^+	5120	414
1^+	218 240	236 595
1^-	31 360	28 991
2^+	120 960	114 016
2^-	145 920 + g.s.	177 802
3^+	60 160	55 355
3^-	53 120	34 836
4^+	-	2797
4^-	30 080	23 897

[8] D. Zinatulina *et al.*, Phys. Rev. C **99**, 024327 (2019).

Results 3/3: OMC vs. $0\nu\beta\beta$ in ^{76}As

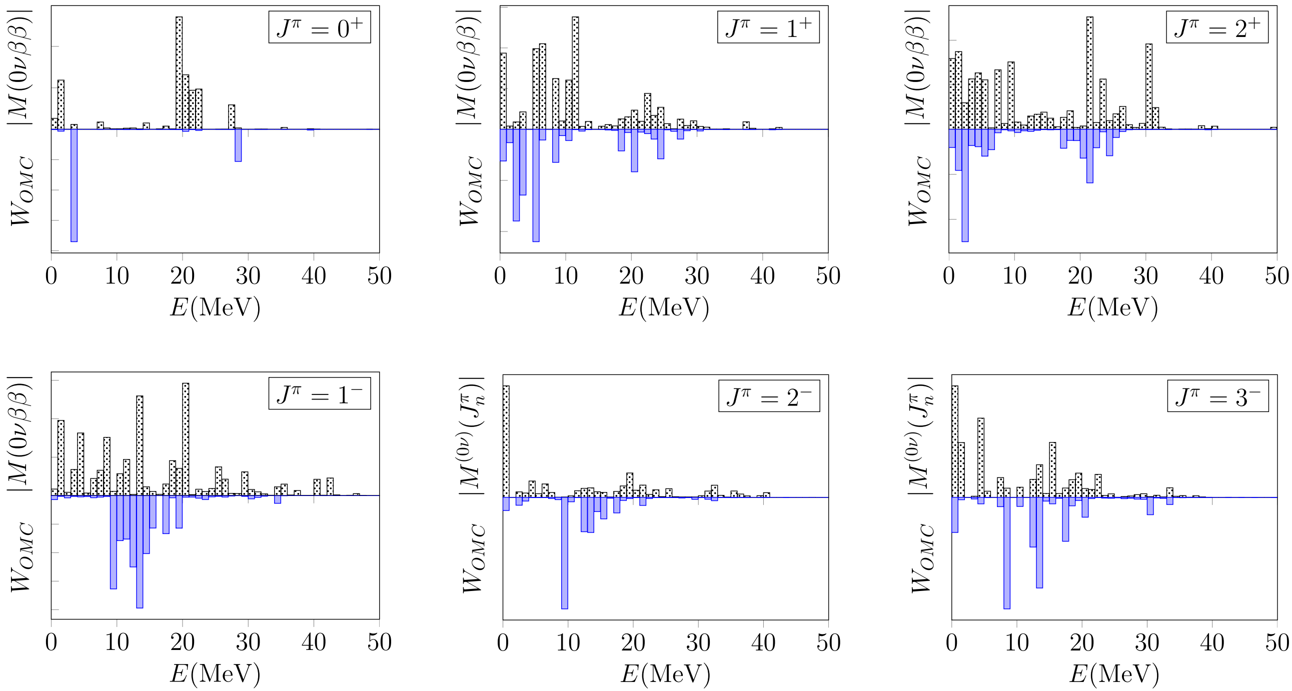

Figure 9: $0\nu\beta\beta$ matrix elements vs. OMC rates to the daughter nucleus of $0\nu\beta\beta$ decay in the A=76 system. J^π refers to the angular momentum of the virtual states of the intermediate nucleus of $0\nu\beta\beta$ decay.

To Be Continued: Muon Capture Rates to the Lowest States of Shell Model Nuclei ^{24}Na, ^{32}P, and ^{56}Mn

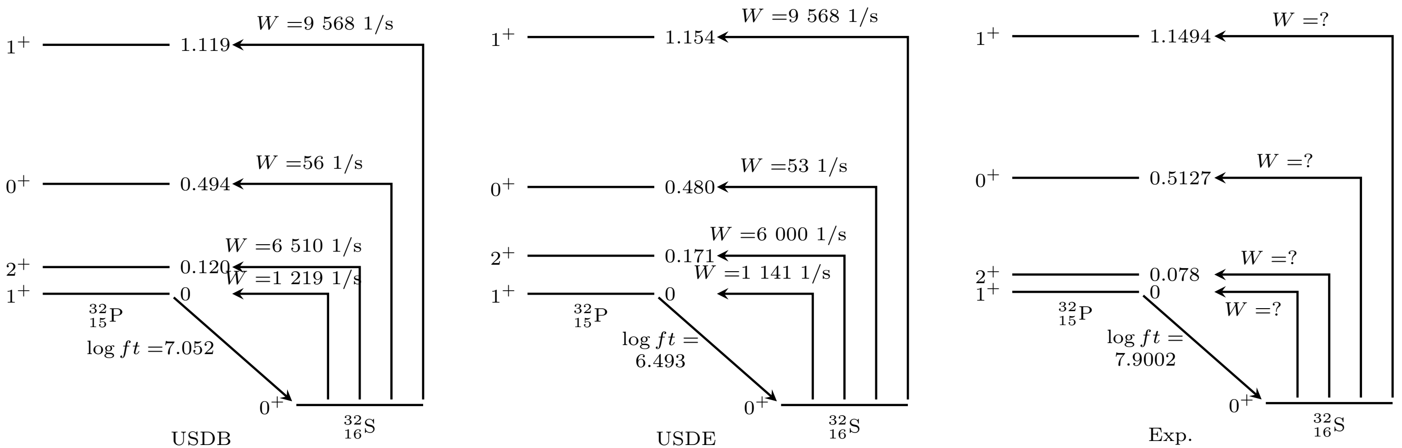

Figure 10: Muon capture rates to the lowest states of ^{32}P computed with two different interactions.

$\rightarrow$ Experiment under planning. $\rightarrow g_A$, g_P?

Summary

- $0\nu\beta\beta$ decay calculations are challenging, and need some complementary tests.

Summary

- $0\nu\beta\beta$ decay calculations are challenging, and need some complementary tests.
- Charge-exchange reactions and nuclear muon capture serve as a useful way to study $0\nu\beta\beta$ decay.

Summary

- $0\nu\beta\beta$ decay calculations are challenging, and need some complementary tests.
- Charge-exchange reactions and nuclear muon capture serve as a useful way to study $0\nu\beta\beta$ decay.
- So far, the theoretical muon capture giant resonances and low-energy OMC rates seem to match the experimental ones.

Summary

- $0\nu\beta\beta$ decay calculations are challenging, and need some complementary tests.
- Charge-exchange reactions and nuclear muon capture serve as a useful way to study $0\nu\beta\beta$ decay.
- So far, the theoretical muon capture giant resonances and low-energy OMC rates seem to match the experimental ones.
- Comparing the total capture rates with Primakoff estimates suggests for strongly quenched g_{A} value.

Summary

- $0\nu\beta\beta$ decay calculations are challenging, and need some complementary tests.
- Charge-exchange reactions and nuclear muon capture serve as a useful way to study $0\nu\beta\beta$ decay.
- So far, the theoretical muon capture giant resonances and low-energy OMC rates seem to match the experimental ones.
- Comparing the total capture rates with Primakoff estimates suggests for strongly quenched g_{A} value.
- We still need more data to be able to fit the parameters g_A and g_P using muon capture results.

Thank you for your attention!